POLYPUBLIE

Suspended whispering gallery mode resonators made of different polymers and fabricated using drop-on-demand inkjet printing for gas sensing applications. Supplément

Marc-Antoine Bianki, Régis Guertin, Cédric Lemieux-Leduc, Yves-Alain Peter

Document en libre accès dans PolyPublie
Open Access document in PolyPublie

Date	2024
Type	Article de revue/Article
Version	Matériel supplémentaire / Supplementary material
URL de PolyPublie **PolyPublie URL**	https://publications.polymtl.ca/59158/
Évaluation par les pairs **Peer reviewed**	Révisé par les pairs / Refereed
Conditions d'utilisation **Terms of use**	Creative Commons Attribution-Utilisation non commerciale-Pas d'oeuvre dérivée 4.0 International / Creative Commons Attribution-NonCommercial-NoDerivatives 4.0 International (CC BY-NC-ND)
Référence **Citation**	Bianki, M.-A., Guertin, R., Lemieux-Leduc, C., & Peter, Y.-A. (2024). Suspended whispering gallery mode resonators made of different polymers and fabricated using drop-on-demand inkjet printing for gas sensing applications. Sensors and Actuators B: Chemical, 420, 136460 (8 pages). https://doi.org/10.1016/j.snb.2024.136460

Publication officielle
Official publication

Titre de la revue **Journal title**	Sensors and Actuators B: Chemical (vol. 420)
Maison d'édition **Publisher**	Elsevier
URL officielle **Official URL**	https://doi.org/10.1016/j.snb.2024.136460
Mention légale **Legal notice**	

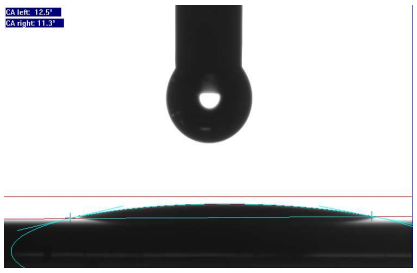
Ce fichier a été téléchargé à partir de PolyPublie, le dépôt institutionnel de Polytechnique Montréal
This file has been downloaded from PolyPublie, the institutional repository of Polytechnique Montréal
https://publications.polymtl.ca

Supplementary materials - Suspended whispering gallery mode resonators made of different polymers and fabricated using drop-on-demand inkjet printing for gas sensing applications

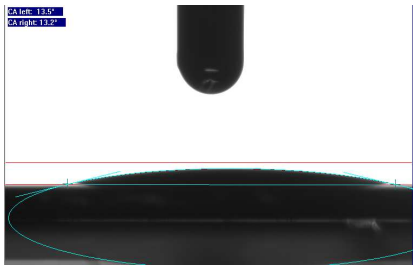
Marc-Antoine Bianki, Régis Guertin, Cédric Lemieux-Leduc, Yves-Alain Peter

[a]*Polytechnique Montréal, 2500 Chem. de Polytechnique, Montréal, H3T 1J4, Qc, Canada*

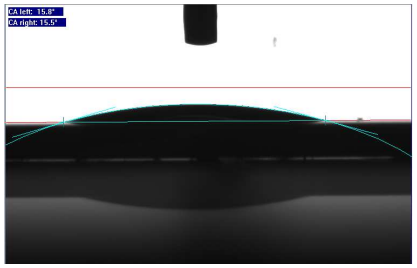
S1. Surface tension



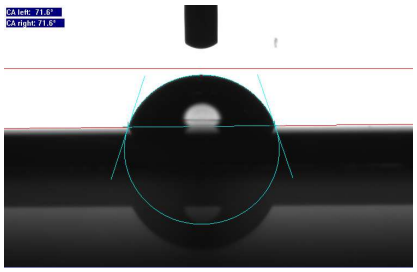
(a) PS on Si ⟨100⟩ substrate treated with a Piranha



(b) PS on Si ⟨100⟩ substrate coated with HMDS



(c) PHMB on Si ⟨100⟩ substrate treated with a Piranha



(d) PHMB on Si ⟨100⟩ substrate coated with HMDS

Figure S1: Optical contact angle measurements with instrument OCA-20 from Data Physics

Table S1: Measured contact angles for the determination of static surface tension of silicon ⟨100⟩ with a Piranha treatment or an HMDS coating as well as PS and PHMB inks

Liquid	Solid	Contact angle (°)
Water	Si ⟨100⟩, Piranha	27.7
	Si ⟨100⟩, HMDS	78.0
Ethylene Glycol	Si ⟨100⟩, Piranha	14.8
	Si ⟨100⟩, HMDS	48.9
Diiodomethane	Si ⟨100⟩, Piranha	42.5
	Si ⟨100⟩, HMDS	53.3
PS in PGMEA (9.9% w/w)	Si ⟨100⟩, Piranha	12.0
	Si ⟨100⟩, HMDS	12.6
PHMB in water (14.3% w/w)	Si ⟨100⟩, Piranha	15.0
	Si ⟨100⟩, HMDS	71.7

Table S2: Total static surface tension (SFT) of different liquids and solids with their dispersion (d) and polar (p) components. Values for water, ethylene glycol and diiodomethane are reported from the literature. Both silicon ⟨100⟩ solids with a piranha treatment and an HMDS coating were measured with the help of the three liquids. Both inks with PS and PHMB were obtained with the measured solids. The static surface tensions were calculated from the contact angles with the Owens, Wendt, Rabel and Kaelble method.

Material	State	SFT (mN/m)		
		total	d	p
Water	Liquid	72.1	19.9	52.2
Ethylene Glycol	Liquid	48.0	29.0	19.0
Diiodomethane	Liquid	50.0	47.4	2.6
Si ⟨100⟩, Piranha	Solid	59.5	15.7	43.8
Si ⟨100⟩, HMDS	Solid	34.1	26.1	8.0
PS in PGMEA (9.9% w/w)	Liquid	33.4	30.6	2.8
PHMB in water (14.3% w/w)	Liquid	61.5	18.3	43.2

S2. Viscosity

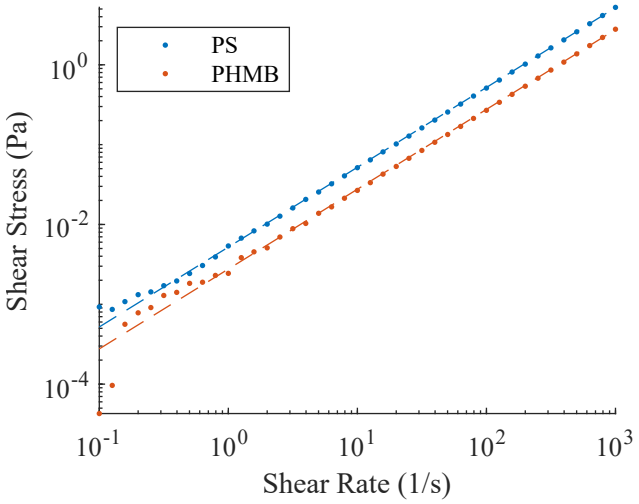


Figure S2: Viscosity measurement of PS and PHMB inks with linear regressions. The slope of the shear stress by the shear rate is the dynamic viscosity. The rotational viscometry measurements were made with the rheometer MCR 501 of Anton Paar with a double-gap spindle DG 26.7 at 25 °C.

S3. Selectivity

Empirical selectivity assessment can be made by computing the selectivity angle between each polymer-analyte pair, calculated as:

$$R_{n,m} = \arccos\left(\frac{\left\langle \vec{S_n}, \vec{S_m} \right\rangle}{\left\| \vec{S_n} \right\| \left\| \vec{S_m} \right\|}\right) \tag{S1}$$

where $\vec{S_n}$ and $\vec{S_m}$ are the selectivity vectors of the analytes n and m with the component of the vectors being the sensitivity of these analytes with each polymer.

The resulting angles serve as a measure of selectivity between two analytes. A measurement of 0° indicates that the two polymers are linearly dependent, rendering the selectivity null, while a measurement of 90° indicates that the two polymers are linearly independent, indicating perfect selectivity. These angles are detailed in Table S3 and fall within a range of a few degrees, indicating low selectivity for these three polymers.

Table S3: Selectivity angles for each pair of gases.

Gas pair	$R_{n,m}$ (°)
IPA - H_2O	7.83
IPA - CO_2	6.22
H_2O - CO_2	3.81

S4. Response Time

Response times were evaluated for each polymer-analyte pair, measuring the normalized peak positions over time during a single transition from the nitrogen blank to the maximum analyte concentration. In Fig. S3, the normalized peak positions are depicted over time, with the change in gas concentration beginning at 0 min. Both the upward transition (from blank to maximum concentration) and the downward transition (from maximum concentration to blank) are illustrated. Two criteria, namely 70 % and 90 % of the total wavelength shift over 60 min, are marked by dashed and dash-dotted vertical lines, respectively, in colors corresponding to the analyte. The overall trend in response time predominantly aligns with the specific polymer and remains similar to the same polymer with different analytes. Consequently, the t_{70} lines closely cluster together, while the t_{90} lines exhibit slightly more spread. Details of the response times are presented in Table S4, revealing that SU-8 exhibits the quickest response time, achieving less than a minute for t_{70}.

The different order of magnitude between the two response time definitions, t_{70} and t_{90} suggests the presence of multiple response regimes. Previous research on the response time of polymer swelling to gas concentration changes has indicated an empirical relationship resembling the summation of two exponential functions, each with different time constants. This model has been applied in the study of materials like polydimethylsiloxane (PDMS) [1] and has been fitted to SU-8 as well [2] and might explain the initial rapid response of PHMB to water vapors, surpassing that of PS (2.5 min>11.8 min), followed by a slower response thereafter (33.5 min<24.7 min).

Since both the downward and upward response times are below 40 minutes, it is confirmed that the sensor has a reversible response at room temperature.

The wavelength shift in time $\Delta\lambda(t)$ can be fit with a two-exponential model where there is a fast and a slow response time with constant τ_1 and τ_2 respectively and $\tau_1 < \tau_2$. The fit equation is:

$$\Delta\lambda(t) = C_0 \pm H(t - t_0)\left(C_1\left(1 - e^{-\frac{t-t_0}{\tau_1}}\right) + C_2\left(1 - e^{-\frac{t-t_0}{\tau_2}}\right)\right) \tag{S2}$$

for upward (plus sign) and downward (minus sign) where $H(t)$ is the Heaviside function, C_1, C_2 and C_0 are proportionality constants and t_0 is the time when the change in concentration occurs. The relative importance of each exponential is given by the ratio between C_1 and C_2.

The three polymers were analyzed with the three analytes. The model fits all experiments well for both upward and downward transitions ($R^2 > 0.977$).

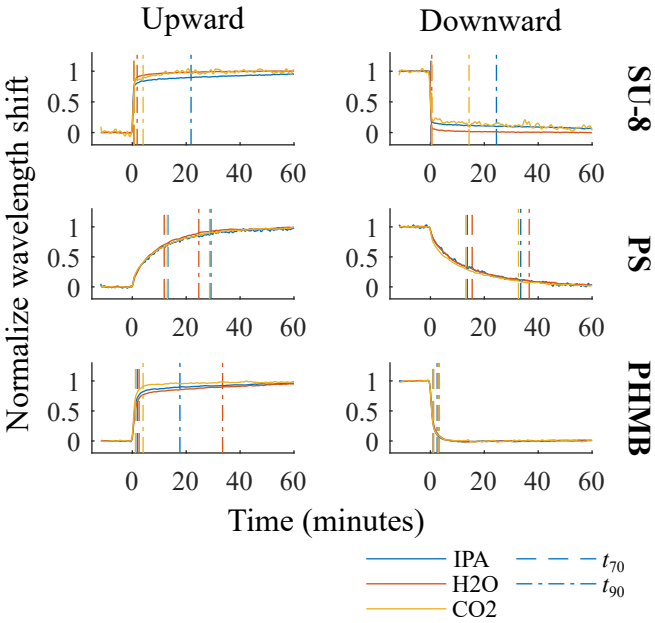


Figure S3: Transient response curves for each polymer-analyte combination, displaying both upward and downward transitions. The response times at 70 % and 90 % of the overall wavelength shifts are indicated by dashed and dash-dotted vertical lines respectively, matching the color code of the corresponding analyte.

Table S4: Response times in minutes for both upward and downward transitions, representing 70 % and 90 % of the maximum wavelength shift for each combination of polymer-analyte pairs.

		t_{70} (minute)			t_{90} (minute)		
		IPA	H2O	CO2	IPA	H2O	CO2
UP	SU-8	0.6	0.6	0.7	21.8	1.8	4.0
	PS	13.2	11.8	13.0	29.2	24.7	28.7
	PHMB	1.8	2.5	1.2	17.7	33.5	4.0
		IPA	H2O	CO2	IPA	H2O	CO2
DOWN	SU-8	0.2	0.3	0.5	24.5	0.5	14.3
	PS	13.7	15.5	13.2	33.5	36.7	32.7
	PHMB	1.0	1.2	1.0	2.5	3.2	2.8

Table S5: Fit results of the sum of two exponential terms for upward and downward transition of each polymer-analyte pair. τ_1 and τ_2 are the fast and slow time constants, R^2 is the coefficient of determination of the fit, and ratio is defined as C_1 divided by C_2.

Polymer	Analyte	Upward				Downward			
		τ_1 (s)	τ_2 (s)	ratio	R^2	τ_1 (s)	τ_2 (s)	ratio	R^2
SU-8	H_2O	10.3	560.8	7.88	1.000	6.0	935.2	19.92	0.999
	IPA	9.5	2550.9	4.67	0.999	6.0	4664.6	5.94	0.999
	CO_2	10.0	521.9	5.30	0.977	10.0	3760.8	4.16	0.975
PS	H_2O	202.8	827.5	0.48	0.999	168.8	1179.1	0.52	0.999
	IPA	167.9	1018.2	0.52	0.991	83.9	1019.5	0.32	0.991
	CO_2	71.1	871.1	0.34	0.999	64.1	977.9	0.44	0.999
PHMB	H_2O	53.1	2353.3	3.33	0.999	19.0	111.1	0.97	0.999
	IPA	44.3	2282.5	4.67	0.999	17.6	102.0	1.35	0.999
	CO_2	33.0	1344.7	8.75	0.997	16.0	118.9	1.56	0.998

References

[1] J. E. Saunders, H. Chen, C. Brauer, M. Clayton, H.-P. Loock, Two distinct mechanisms upon absorption of volatile organic compounds into siloxane polymers, Soft Matter 14 (12) (2018) 2206–2218. doi:10.1039/c7sm02234d.

[2] C. Lemieux-Leduc, R. Guertin, M.-A. Bianki, Y.-A. Peter, All-polymer whispering gallery mode resonators for gas sensing, Optics Express 29 (6) (2021) 8685. doi:10.1364/oe.417703.